J Plant Biotechnol (2022) 49:257-270
DOI:https://doi.org/10.5010/JPB.2022.49.3.257

ISSN 1229-2818 (Print)
ISSN 2384-1397 (Online)

Research Article

Antimicrobial polyhydroxybutyrate submicron fiber mat loaded with extract of *Hypericum perforatum*

Milos Beran · Ales Horna · Viktor Vorisek · Eliska Berkova · Radka Korinkova · Vojtech Trousil · Marketa Hrubanova

Received: 15 February 2022 / Revised: 23 June 2022 / Accepted: 23 June 2022

Abstract The aim of this work was to prepare a new biodegradable polyhydroxybutyrate (PHB) submicron fiber mat loaded with hypericin-rich *Hypericum perforatum* raw extract by centrifugal spinning technology, an alternative approach to the traditional method of electrospinning to fabricate nanofibers or microfibers from solutions at high speed and low cost. Hypericins in methanol/acetone extract of *H. perforatum* were determined by UHPLC-MS/MS and HPLC/PDA. Submicron fiber mats composed of pure PHB or PHB enriched with H. perforatum extract were prepared using a pilot plant demonstrator for the centrifugal spinning technology and characterized by SEM. Singlet oxygen production was quantified by the 1,3-diphenylisobenzofuran (DPIBF) method in hexane. The results proved a significant production of singlet oxygen by the prepared submicron fiber mat. We also found a significant antibacterial activity against the bacterial strain *Escherichia coli* CCM 5417 by a method in accordance with JIS Z 2801/ISO 22196 standards. The *H. perforatum* extract-enriched PHB submicron fiber mats showed potential for the development of self-cleaning and antimicrobial air filters.

Keywords Hypericum perforatum, Hypericin extract, Polyhydroxybutyrate, Submicron fiber, Singlet oxygen, Antimicrobial air filter

M. Beran (✉) · E. Berkova
Food Research Institute Prague, CZ10200 Prague, Czech Republic
e-mail: mb.ontheroad@seznam.cz

A. Horna · V. Vorisek
Radanal Ltd., CZ53003 Pardubice, Czech Republic

R. Korinkova · V.Trousil
Centre of Organic Chemistry Ltd., CZ53354 Rybitví 296, Czech Republic

M. Hrubanova
Textile Testing Institute, CZ602 00 Brno, Czech Republic

Introduction

Hypericum is a genus of flowering plants in the family *Hypericaceae*. There are over 490 species in the genus. *Hypericum perforatum*, known as perforate St John's-wort, common Saint John's wort, or simply St John's wort, is the most commonly used and best studied species of the genus. It can be found across temperate areas of Eurasia and has been introduced as an invasive weed to much of North and South America, as well as South Africa and Australia. The perennial flowering plant has been used medicinally for thousands of years, and remains commercially cultivated in the 21st century. It was thought to have medical properties in classical antiquity and was a standard component of theriacs, from the Mithridate of Aulus Cornelius Celsus' De Medicina (ca. 30 CE) to the Venice treacle of d'Amsterdammer Apotheek in 1686. Folk usages included oily extract ("St John's oil") and ethanolic extracts. The red, oily extract of *H. perforatum* has been used in the treatment of wounds, including by the Knights Hospitaller, the Order of St John, after battles in the Crusades, which is most likely where the name derived. Besides treatment of cuts and burns it has been utilized to mitigate symptoms of anxiety and depression. Recent research suggests the effectiveness of this herb in treating other ailments, including cancer, inflammation-related disorders, and bacterial and viral diseases, and as an antioxidant, anti-inflammatory and neuroprotective agent. Pharmaceutical companies, particularly in Europe, prepare standard formulations of this herb that are taken by millions of people. Nearly two dozen of bioactive compounds have been isolated from the herb (Schwob et al. 2002; Tatsis et al. 2007). Hyperforin, hypericin ant their derivatives have been identified as the main bioactive components (Umek et al. 1999). Hyperforin has only been found in significant amounts in *H. perforatum* with other related species such as *Hypericum calycinum*

containing lower levels of the phytochemical. Hyperforin has been shown to be a major antidepressant component in the extract of *H. perforatum* (Zanoli 2004). The major bioactive constituent acts in several ways: serving as a neurotransmitter reuptake inhibitor with a broad selectivity, as a ligand for the pregnane X receptor, and as an antibacterial and antitumor agent (Bouron and Lorrain 2014; Gharge et al. 2009). Hypericin is a naturally occurring chromophore found in some species of the genus *Hypericum*, especially *H. perforatum L.* (St. John's wort), and in some basidiomycetes (*Dermocybe spp.*) or endophytic fungi, such as *Thielavia subthermophila* (Jendzelovska et al. 2016). Chemically, hypericin is an aromatic polycyclic dione with a molecular mass of 504.4 Da and belongs to the naphthodianthrone family. The aromatic rings of hypericin confer photochemical properties on this plant pigment, which has a broad absorbance spectrum with maxima at 545 and 595 nm and a wide range of emission wavelengths peaking at 594 and 640 nm (Ayane et al. 2015). Hypericin and its derivatives belong to the group of photosensitizers together with phthalocyanines, porphyrins, chlorins, bacteriochlorins, phenothiazines, halogenated xanthenes, perylenequinones, and other synthetic dyes. Their maximum light absorption occurs in the visible portion of the electromagnetic spectrum, which constitutes a larger portion of the spectrum and thus more available than the ultra-violet portion required by other sensitizers. Photocatalysis has been recognized as a promising technique for water and air purification and disinfection and has since been studied extensively as an alternative to currently used technologies, such as chlorination, ozonation and adsorption on active carbon (Zugle et al. 2012). Singlet oxygen is an extremely effective agent for complete oxidation of common organic pollutants of water including chlorinated phenols. Increasing antimicrobial resistance to antibiotics requires the development of novel materials and approaches, such as photodynamic therapy and inactivation, for treatment of various infections. Such materials, including hypericin, can be potentially used in antibacterial therapy of chronic wounds, infections of diabetic ulcers, and burns, as well as rapidly spreading and intractable soft-tissue infections caused by resistant bacteria (Severyukhina et al. 2017). Singlet oxygen production by photo-excited hypericin dissolved in dimethyl-sulfoxide (DMSO) was studied by means of time-resolved phosphorescence measurements. The obtained quantum yield of singlet oxygen photosensitized by hypericin in air-saturated DMSO is $\Phi\Delta = 0.4 \pm 0.03$ (Varchola et al. 2016). Naphtodianthrones isolated from the genus *Hypericum* include hypericin, pseudohypericin, and isohypericin. So-called protoderivatives, protohypericin and protopseudohypericin, lacking the 4,4′-bonds, have been isolated from fresh plant material and they represent the biosynthetic precursors of the more stable compounds, hypericin and pseudohypericin, respectively. Their conversion is catalysed by light. Cyclopseudohypericin, an oxidation product derived from pseudohypericin, has also been isolated (Wirz et al. 2001). Onoue et al. (2011) characterized photobiochemical properties of the constituents of *H. perforatum* extract with focus on generation of reactive oxygen species (ROS), lipid peroxidation, and DNA photo-cleavage. Concomitant UV exposure of quercitrin, and component with potent UV/Vis absorption, with hyperforin resulted in significant attenuation of photodynamic generation of singlet oxygen from hyperforin, but not with hypericin. However, aforementioned photocatalytic properties of hyperforin have never been confirmed from other sources. Both hypericin and hyperforin are under study for their potential antibiotic properties. The singlet oxygen or other ROS can cause damage to bacterial cells or other microbes through several mechanisms. These include oxidation of membrane lipids and amino acids in proteins, cross-linking of proteins and oxidative damage to nucleic acids with the subsequent disturbance of the normal functioning of the pathogen (Luksiene 2003). Schempp et al. (1999) reported the antibacterial activity of hyperforin from *H. perforatum* against multiresistant *Staphylococcus aureus* and other gram-positive bacteria. The effectiveness of hypericin-mediated photodynamic killing was reported to be strongly affected by cellular structure and photosensitizer uptake. The combination of hypericin and light irradiation could induce significant killing of gram positive methicillin-sensitive and -resistant *Staphylococcus aureus* cells (> 6 log reduction), but was not effective on gram negative *Esherichia coli* cells (< 0.2 log reduction). The difference was caused by different cell wall/membrane structures that directly affected cellular uptake of hypericin (Yow et al. 2012). Significant photodynamic antibacterial activities of *H. perforatum* extracts against both planktonic and biofilm-forming *Staphylococcus aureus* bacteria have been reported repeatedly (Delcanale et al. 2020; Garcia et al. 2015). Other authors (Avato et al. 2004) assayed extracts prepared with different solvents from the aerial parts of *H. perforatum* against different microorganisms. Growth inhibition was observed only for gram-positive bacteria, *Bacillus subtilis* and *Bacillus cereus* being the most susceptible to the tested drugs. The extract obtained with ethyl acetate was the most active. The main constituents of this extract, as determined by HPLC analysis, were flavonoids, hypericins and hyperforins. Hypericin, hyperforin and its stable

dicyclohexilammonium salts were identified as the active agents. Flavonoids appeared inactive at all. A comprehensive summary of the ethnobotanical uses, chemical constituents and biological effects (antibacterial and antifungal) of *H. perforatum* was reviewed (Saddiqe et al. 2010). The available literature indicates that it has a higher antibacterial activity against gram-positive than gram-negative bacteria, and alcoholic extracts (methanolic/ethanolic) were shown to possess more pronounced activity than aqueous extracts. However, Milosevic et al. (2007) observed extreme sensitivity of gram-negative bacteria *Pseudomonas glycinea* and *Azotobacter chrococcum* on an ethanolic extract of *H. perforatum*, while no effect was observed on another gram-negative bacteria *Klebsiella pneumoniae*. Antimicrobial activities of *H. perforatum* extracts or hypericins against pathogenic fungi and spoilage yeasts have also been reported. Significant reduction of the number of *Fusarium oxysporum* and *Penicillium canescens* spores was observed after application of an ethanolic extract of *H. perforatum* (Milosevic et al. 2007). In vitro fungicidal photodynamic effect of hypericin on *Candida* species described Rezusta et al. (2012). In another experimental work antifungal properties of hypericin, hypericin tetrasulphonic acid and fagopyrin, which is analogue of hypericin, against a set of pathogenic fungi and spoilage yeasts including: *Microsporum canis*, *Trichophyton rubrum*, *Fusarium oxysporum*, *Exophiala dermatitidis*, *Candida albicans*, *Kluyveromyces marxianus*, *Pichia fermentans* and *Saccharomyces cerevisiae* were determined (Sytar et al. 2016). Both light-dependent and light-independent antiviral *in vitro* and *in vivo* activities of hypericins and other components of *H. perforatum* extracts against different types of viruses have been described. Hypericin readily inactivated murine cytomegalovirus, *Sindbis virus* (Hudson et al. 1991; Lopez-Bazzocchi et al. 1991), and human immunodeficiency virus type 1 - HIV-1 (Birt et al. 2009; Hudson et al. 1991; Lopez-Bazzocchi et al. 1991) in a dose-dependent manner, especially on exposure to fluorescent lighting. The antiviral activities of *H. perforatum* ethyl acetate extract on infectious bronchitis virus were evaluated. Significant effects were observed both in vitro and in vivo. Hyperoside, quercitrin, quercetin, pseudohypericin, and hypericin were identified as the main active agents and a combination of these compounds could mediate the antiviral activities (Chen et al. 2019). Some plants of the genus *Hypericum* from Southern Brazil contain compounds with potential antiviral activity against lentiviruses (Schmitt et al. 2001). *H. perforatum* extract was effective against influenza A virus in vitro (Pu et al. 2009). However, no detectable anti-hepatitis C virus (HCV) activity in patients with chronic HCV infection was detected (Jacobson et al. 2001). Activity of *H. perforatum* extracts against many types of viruses, especially coronavirus family (Kim et al. 2019), gives us a hope and also supports the postulation that the herb may help in delaying the progression of covid-19 infection (Eldeeb and Belal 2020). Recently, naturally occurring anthraquinones became one of the „irons in the fire“ in the fight against the novel SARS-CoV-2 virus as potential inhibitors of the virus main papain-like protease, important for blocking the viral replication of the virus and further spread of the infection (Das and Singha Roy 2020; Islam et al. 2021; Pitsillou et al. 2020a, b), and other important antiviral drug targets (Balmeh et al. 2020; Liu et al. 2021; Smith and Smith 2020). Further studies are needed to let these herbal medications turned into practice. Photodynamic therapy, that involves the use of photosensitizing agents along with light of an appropriate wavelength to generate cytotoxic reactive oxygen species, is an innovative approach to treat diverse cancers, too. Hypericin is a powerful natural photosensitizer that is applicable in the photodynamic therapy (PDT) of various oncological diseases. As the accumulation of hypericin is significantly higher in neoplastic tissue than in normal tissue, it can be used in photodynamic diagnosis (PDD) as an effective fluorescence marker for tumour detection and visualization. In addition, light-activated hypericin acts as a strong pro-oxidant agent with antineoplastic and antiangiogenic properties, since it effectively induces the apoptosis, necrosis or autophagy of cancer cells with minimal dark toxicity (Head et al. 2006; Liu et al. 2015; Miskovsky 2002). Different extraction procedures have been evaluated to quantify the major constituents (hypericins, hyperforins and flavonoids) of *H. perforatum* drug samples. Sonication with methanol resulted in the best extraction method to obtain a homogenous drug sample, representative of all the major metabolites and with less degradation of products (Avato and Guglielmi 2008). Highest amounts of hypericins were extracted by ultrasonic methods using methanol: acetone 2:1 (Ramezani and Zamani 2017), and mixture of 50:50 v/v ethanol and methanol (Tahmasebi-Boldaji et al. 2019) as extracting solvents. Microwave activation was found reducing the time necessary to fully extract the naphthodianthrone pigments from *H. perforatum* compared to classical extraction. The maximal pigment extraction was found to be achieved when using 55% ethanol or isopropanol as extractants using microwave activation (Punegov et al. 2015). The sample gathered at the end of the blossoming extracted with nonpolar solvent (sc-CO2)

at mild temperature (40°C) provided stable hyperforin rich extract. The sample gathered at the beginning of the blossoming extracted with polar solvent (ethanol) at mild temperature (40°C) provided stable hypericin rich extract. High hyperforin yields were obtained with other nonpolar solvents, such as hexane, too (Cossuta et al. 2012). Other advanced techniques utilized to extract hypericins from *H. perforatum* are: supercritical fluid extraction (Cossuta et al. 2012), pressurized liquid extraction (Williams et al. 2006), accelerated solvent extraction (ASE), and pressured water extraction (Koturevic et al. 2021). *H. perforatum* herbal preparations are generally standardized to "total hypericins". The current standard method for determining the naphthodianthrone content is a spectrophotometric method specified in the United States Pharmacopeia. However, compounds other than hypericin and pseudohypericin can contribute falsely to the naphthodianthrone concentration, reducing this methods specificity (Draves and Walker 2003). Photocatalysts may be deactivated by the oxidative self-destruction during the catalytic oxidation. To solve these problems, numerous support materials can be employed to immobilize the photocatalytic molecules to prepare the heterogeneous catalysts. The immobilization of photocatalysts can eliminate costly and impractical post-treatment recovery of spent photocatalysts in large scale operations. Factors such as high durability, ease of availability, low density, chemical inertness and mechanical stability are primary factors responsible for the selection of suitable supports for catalysts (Srikanth et al. 2017). Nanostructured materials are ideal candidates as immobilization agents, because of the large surface area to volume ratios. Moreover, nanofibrous supports show many advantages for their high porosity and interconnectivity. The spectroscopy and photophysics of several hypericin were studied in methanol and when bound to liposomes. The singlet oxygen quantum yields ΦΔ 0.39+/-0.01 in methanol, and 0.35+/-0.05 in lecithin vesicles were reported (Roslaniec et al. 2000). Thermosensitive liposomes encapsulating hypericin prepared and characterized by Dayyih et al. 2021. Stable dipalmitoylphosphatidylcholine (DPPC) liposomes coated with F127 copolymer for hypericin loading and delivery described Morais et al. (2020). Phosphorescence kinetics of singlet oxygen production by in hypericin molecules inside low-density lipoprotein particles has also been studied recently (Datta et al. 2018). Hypericin-loaded solid lipid nanoparticles for usage in photodynamic therapy were described by other authors (Lima et al. 2013). Hypericin loading to lipid nanocapsule formulations increased its apparent solubility and enhanced the production of singlet oxygen (Barras et al. 2013). Kubin et al. (2008) developed an aqueous solution of hypericin non-covalently bound to polyvinylpyrrolidone suitable for diagnostic and therapeutic applications. The novel preparation of hypericin bonded with poly-n-vinylamides, especially polyvinyl pyrrolidone, has also been patented (Kubin and Loew 2004). The water-soluble formulations of hypericin with polyvinyl pyrrolidone, which could be applied as aqueous sprays, were successfully tested for their efficiency in killing *Staphylococcus aureus* (Abdelhamid et al. 2020; Engelhardt et al. 2010). Other authors nanoencapsulated hypericin in Pluronic® P123 (a copolymer comprising polyethylene oxide and polypropylene oxide) and used it for photodynamic therapy of dermatophytosis (Galinari et al. 2021). Malacrida et al. (2020) proved hypericin-mediated photoinactivation of polymeric nanoparticles against *Staphylococcus aureus* bacteria. An alternative treatment approach for onychomycosis caused by *Fusarium* spp. using hypericin-P123 photodynamic therapy described Conrado et al. 2021. *H. perforatum* extract encapsulated in poly(lactic-co-glycolic acid) (PLGA) nanoparticles can successfully and specifically target esophageal squamous carcinoma cells (Amjadi et al. 2019). The cellular uptake and phototoxicity of hypericin was enhanced by encapsulation into surface coated zein formulations (Abdelsalam et al. 2021). The formation of the inclusion complexes between β-cyclodextrin and constituents of ethanolic extracts of *H. perforatum* was also confirmed (Kalogeropoulos et al. 2008). Photosensitizers can be embedded in polymeric fibers being spun directly by simple addition into the polymeric solution or with a covalent bond so that they could not escape spontaneously from the filtration materials (Kimmer et al. 2012). The photosensitizers can also be anchored to the fiber surface, usually by a covalent bond, as such, or in a form of a complex or a conjugate prepared earlier. Evaluation of poly ε-caprolactone electrospun nanofibers loaded with *H. perforatum* extract as a wound dressing has been described. These unique structures were very useful as burn and ulcer dressings (Pourhojat et al. 2017). Antibacterial electrospun poly lactic-co-glycolic acid nanofibers containing *H. perforatum* extract with satisfactory drug release performance were successfully tested for bedsore healing (Pourhojat et al. 2018). Electron donor properties of hypericin have also been utilized for sensitization of inorganic semiconductors, such as TiO_2, to enhance its photodynamic activity in the visible light region. TiO_2 nanoparticles doped with Zn and hypericin were used in the treatment of cutaneous leishmaniasis caused by *Leishmania*

Table 1 UHPLC-MS/MS gradient and flow rates

Time (min)	0	2	5	12	14.I	20
Flow rate (ml·min^{-1})	0,4	0,4	0,5	0,5	0,4	0,4
Eluent B (%)	2	55	100	100	2	2

amazonensis (Lopera et al. 2020; Sepúlveda et al. 2020). Moreover, hypericin was tested for sensitization of nanoporous TiO_2 electrodes in TiO_2-based photovoltaic cells (Johnston et al. 2001) and in the TiO_2 photoanode of dye sensitized solar cells (Cvetanovic Zobenica et al. 2019). The aim of this work was to prepare a new biodegradable polyhydroxybutyrate submicron fiber mat loaded with *H. perforatum* hypericin rich raw extract by centrifugal spinning technology, an alternative approach to fabricate nanofibers or microfibers from solutions at high speed and low cost.

Materials and Methods

Hypericum perforatum herb extraction

Wild growing *H. perforatum* herbs were collected in surrounding of Food Research Institute Prague, Czech Republic, at the turn of July and August 2020. To prepare hypericins (naphthodianthrones) rich extract, we have adopted and slightly modified the extraction method from Ramezani and Zamani 2017. The leaves were dried at room temperature for about 14 days. Then, they were grinded and kept in a dark glass bottle before extraction. Chlorophylls and some unwanted nonpolar components of the leaves were removed using chloroform as a solvent. To do so, about 10 g of leaf powder was poured into a dark glass, 50m mL of dichloromethane chloroform was added, the mixture was put in an ultrasonic bath for about 30 minutes, extracted at 40°C overnight and was then filtered with a paper filter. The supernatant, containing unwanted compounds, were discarded. Then, 240 mL of methanol : acetone (2:1 w/w) was added to the plant residue, sonicated for about 30 minutes, extracted at 40°C overnight and was then filtered with a paper filter. The red supernatant was kept in a dark glass bottle. The extraction was repeated two times adding 240 mL portions of the above mentioned solvent on the plant residue. Both the portions were mixed and the solvents were evaporated to dryness under vacuum. All reagents were of analytical grade. Methanol, acetone, chloroform were purchased from VWR (Stříbrná Skalice, Czech Republic).

Spectroscopic characterization of the extract

Vis absorption spectra of hypericin analytical standard purchased from HWI Pharma Services GmbH (Rülzheim, Germany) and our dried extract were measured using Tecan Infinite M200 Plate Reader (Tecan Group Ltd., Männedorf, Switzerland). The standard sample was dissoluted in dimethyl sulfoxide (Merck, Prague, Czech Republic) in concentration 1 mg.l^{-1}, samples of the dried extract in concentrations 10 and 200 mg.l^{-1}.

Determination of hypericins by UHPLC-MS/MS

The dried samples of hypericins rich extract of *H. perforatum* were kept in a freezer at temperature -18°C. All experiments were carried out under dark. The hypericin analytical standard purchased from HWI Pharma Services GmbH (Rülzheim, Germany) and dried hypericins rich extract were dissolved in solution of 0,1% (v/v) formic acid in water/methanol, 1/1 (v/v) to reach concentration 0,25 mg.ml^{-1}. After thorough dissolution, the solution of the extract was filtered using Munktell Ahlstrom filtration paper for quantitative analysis with 1 - 2 μm capture efficiency (Verkon, Prague, Czech Republic). The UltiMate 3000 Binary RSLC chromatograph equipped with the TSQ Quantum Access Max Triple Quadrupole Mass Spectrometer (Thermo Fisher Sc., Prague, Czech Republic) was used for analysis of the extracts. Extract separation was carried out on the Kinetex 1,7 μm F5 100 Å, 50 × 2,1 mm, chromatographic column (Chromeservis, Prague, Czech Republic) using elution with 0,1% (v/v) formic acid in water (A) and acetonitrile with methanol (1:1, v/v) with addition of formic acid (B) with flow rates and gradient shown in Table 1.

Determination of hypericins by UHPLC/PDA

UltiMate 3000 Binary RSLC chromatograph equipped with the Surveyor photo diode array PDA Plus Detector (Thermo Fisher Sc.) was used for chromatographic analysis of the extracts. Flow rate was 1 ml·min^{-1} and oven temperature 40°C. Gradient elution was performed with 0,5M acetic acid (eluent A), 100% methanol (eluent B), and 100% acetonitrile (eluent C) according the scheme

Table 2 UHPLC/PDA gradient

Time (min)	0	0,1	0,5	3	3,1	5	5,1	7	7,1	8	10
Eluent B (%)	2	5	55	55	10	10	10	5	2,5	2	2
Eluent C (%)	0	5	5	6	15	30	35	0	0	0	0

Table 3 Parameters of the fiber forming process

Rotation speed of the fiber-froming disc	4200 rpm
Solution flow rate	12 ml/min
Air flow rate	71 m3/h
Input air temperature	24°C
Rotation speed of the fiber collector	5500 rpm

Fig. 1 Preparation of the PHB submicron fiber mat by the centrifugal spinning technology and a rotating fiber collector

shown in Table 2. Hypericin from *H. perforatum* produced by Fluka, 95% (HPLC grade), was used as an inner standard for hypericins determination. All solvents and chemicals of p.a. grade were purchased from VWR (Stříbrná Skalice, Czech Republic).

Preparation of the PHB submicron fiber mat enriched by the extract

The NANOCENT demonstrator (DBH Technologies, Cerncice, Czech Republic) for the centrifugal spinning technology was used to produce the polyhydroxybutyrate (PHB) (Biomer, Krailling, Germany) submicron fiber mats. The demonstrator is based on a new method for preparation of submicron fibers and can be adjusted to produce various types of fiber membranes and 3D constructs for use in wide spectrum of industry applications. The submicron fiber production is based on improved centrifugal technology (Beran et al. 2017), using a fiber-forming conical hollow disc, composed from lower and upper parts forming an inner space with an outlet gap in-between them, connected with a hollow shaft and rotating around the axis at 1500 - 5000 rpm. Via openings a polymeric solution is sprayed from an inner space of the hollow shaft to the inner space of the rotating disc. The fibers are formed by centrifugal force at the edge of the outlet gap and collected in form a homogenous mats on a cylindrical collector positioned beside the fiber-forming disc and rotating at 1000 - 12000 rpm (see Fig. 1). For these experiments, 2% (w/w) solution of the PHB polymer in chloroform was prepared. PHB was dissolved at 70°C under continual shaking for 48 hours. A concentrated *H. perforatum* extract solution in methanol : acetone (2:1, w/w), containing 14,8% (w/w) of dry matter, was added to the PHB chloroform solution to reach 0,3% (w/w) final concentration of the extract components in the resulting solution. Parameters of the fiber forming process are summarized in Table 3.

Characterisation of the PHB submicron fiber mats by Scanning Electron Microscopy

Scanning Electron Microscopy (SEM) was used to analyse the particle sizes and morphologies. The samples of the fibers were fixed with a double-faced adhesive tape to the holders and evaluated in a Phenom G2 scanning electron microscope (Phenom-World BV, Eindhoven, Netherlands).

Quantification of singlet oxygen production by the extract and the PHB submicron fiber mats enriched by the extract

Indicator 1,3-diphenylisobenzofuran (DPIBF) reacts with intermediate singlet oxygen $^1O_2$, forming an unstable peroxide that decomposes into colourless 1,2 dibenzoylbenzene (see Fig. 2). The method is selective for determination of

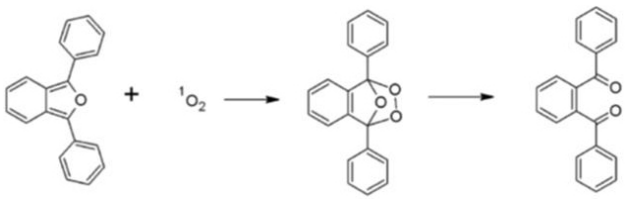

Fig. 2 Scheme of reaction 1,3-diphenylisobenzofuran (DPIBF) indicator with intermediate singlet oxygen $^1O_2$ resulting in formation of an unstable peroxide that decomposes into colorless 1,2-dibenzoylbenzene

singlet oxygen $^1O_2$ production (O'Neill et al. 2003). No other reactive oxygen forms affect the result. The reaction rate was followed by measurement of light absorbance at λ = 415 nm, when absorbance decrease occurs because of the reaction of the indicator with singlet oxygen $^1O_2$ in dependence on the light energy emitted from a light source. On the basis of characteristics of absorption spectrum of hypericins in the visible region, Narva Yellow fluorescent tube, 36W, T8 (Sterix, Prague, Czech Republic) was chosen as a light source for the experiments. Characteristics of the fluorescent tube were determined using Red tide USB 650 UV fiber spectrometer (GMP, Fällanden, Switzerland) at 4 cm distance, corresponding the conditions in the real experimental setup. Resulting radiant flow 156 μW, radiation intensity 13 μW/cm^2 and energy 2,74.10^{14} eV have been determined. Singlet oxygen $^1O_2$ productions by a hypericin standard (HWI Pharma Services GmbH, Rülzheim, Germany) and the dried *H. perforatum* extract were measured in dimethyl sulfoxide (DMSO) solvent (Merck, Prague, Czech Republic) in concentration 1 mg·ml^{-1} at 4 cm distance from the light source. The measurements were carried out in 1x1 cm cells. DPIBF (Merck, Prague, Czech Republic) in a stock solution was added to the DMSO solvent before the measurement to reach absorbance $A_{415} \approx 1{,}0$ (c ~2g/l). On the basis the obtained linear graphical representation of dependence A_{415} = f(t), slopes k and corresponding half-times of DPIBF indicator decomposition $\tau_{1/2}$ were determined. The obtained values of k and $\tau_{1/2}$ were corrected against the slope of decomposition of pure DPIBF indicator (control) to obtain k_{corr} and corresponding $\tau_{1/2corr}$ values.

To measure singlet oxygen $^1O_2$ production of the control pure PHB and *H. perforatum* functionalized PHB nanofiber mats, similar procedure was used. For the measurement, DMSO solvent was replaced with hexane (Merck, Prague, Czech Republic). Hexane was chosen as a nonpolar solvent because it can dissolve the DPIBF indicator, but PHB and the component of the extract are insoluble in it. Moreover, the molar ratio of the absorbed oxygen is even higher than in water. Samples of the nanofiber mats 7 × 7 mm were put into measurement cells instead the hypericin standard and extract samples. To obtain k_{corr} and corresponding $\tau_{1/2corr}$ values for the *H. perforatum* functionalized PHB nanofiber mat, the resulting k and $\tau_{1/2}$ values were corrected both against the slope of decomposition of pure DPIBF indicator and pure PHB nanofiber mat control. All experiments were carried out in triplicate.

Determination of the antibacterial activity of samples of the submicron fiber mat loaded with the extract

To determine the antimicrobial effects of the fiber mats loaded with the photosensitizer, bacterial strain *Escherichia coli* CCM 4517 was chosen as a typical representative of gram-negative bacteria. The bacterial strain was purchased from the Czech Collection of Microorganisms, Brno, Czech Republic. Antibacterial (antimicrobial) activity of surfaces of materials is tested in accordance with JIS Z 2801/ISO 22196 certified method. This internationally recognized test was modified by Textile Testing Institute (Brno, Czech Republic) for determination of antimicrobial activity of photocatalytic surfaces. Briefly, the PHB fiber mats, without (control) and with the *H. perforatum* extract, were cut into squares of 50 mm ± 2 mm. Before the experiments, the squares of the fiber mats were sterilized by gamma-irradiation, using the basic sterilization dose (Microtron MT25, Nuclear Physics Institute, Academy of Sciences of the Czech Republic, Řež). Each of the sterile squares of the fiber mats was placed in a sterilized Petri dish making the test surface up. Exactly 0.4 ml of the test inoculum in form of a suspension of the test bacteria in a 500x diluted nutrient broth (final bacterial concentration for testing was 7,96.10^3 CFU/ml) was pipetted onto the surface of the test material. Thereafter the piece with the test inoculum was covered with a square of HDPE foils of (40 ± 2) mm, the foil was pressed so that the test inoculum spreads over the foil while paying attention so that the inoculum does not spill over from the edge of film, and the lid of the Petri dish was placed on (see Fig. 2). The Petri dishes containing the test pieces inoculated with the test inoculum were incubated at a temperature of (35 ± 1)°C and a relative humidity of not less than 90% for (24±1) h in the ATLAS lightbox, equipped by two ATLAS 56001660 tubes, l = 120 cm, power 36 W, providing D65 light. D65 roughly corresponds to the colour temperature of the sky on a clear day around noon. Light intensity on the sample surface was (1150 ± 100) lx. The samples were incubated in triplicate under the standard illuminant and unlighted (control). Surviving bacteria in the washings

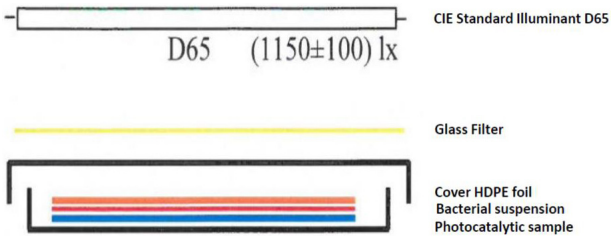

Fig. 3 Scheme of the modified JIS Z 2801 assay setup

Fig. 4 *H. perforatum* herb extraction with chloroform (left) and methanol : acetone (2:1 w/w) (right)

were counted to evaluate the antimicrobial activity of the test material. Counts were determined before and after incubation by standard plate count agar cultivation on Petri dishes at 37°C and relative humidity (95 ± 2)%. Using a formula provided bellow, the log of the difference between the two counts is determined to give a measurement of antimicrobial activity. Difference in between the lowest and the highest result in the triplicate measurements must not exceed 1 log, otherwise the test has to be repeated.

The antibacterial activity R was calculated according to the formula: $R = (U_t - U_0) - (A_t - U_0) = U_t - A_t$ where, R is antibacterial activity; U_0 is an arithmetic average of common logarithms of viable bacteria (CFU), determined with 3 control PHB samples immediately after inoculation; U_t is an arithmetic average of common logarithms of viable bacteria (CFU), determined with 3 control PHB membrane samples after 18 h of incubation; A_t is an arithmetic average of common logarithms of viable bacteria (CFU), determined with 3 experimental PHB - *H. perforatum* samples after 18 h of incubation.

Results and Discussion

Hypericum perforatum herb extraction

Photographs of prepared *H. perforatum* chloroform and methanol/acetone (2:1 w/w) extracts are shown in Fig. 4.

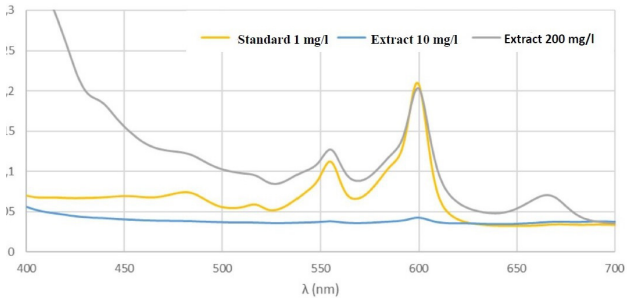

Fig. 5 Vis absorption spectra of the extract in comparison with hypericin standard

The green chloroform containing chlorophylls and some unwanted nonpolar components was discarded. The red methanol/acetone extract was used for following experiments.

Spectroscopic characterization of the extract

Vis absorption spectra of the extract in comparison with hypericin standard in DMSO are shown in Fig. 5. Characteristic peaks of hypericin at approximately 560 and 600 nm are noticeable on the Vis absorption spectra of the extract with excellent correspondence with the spectrum of the standard. The peak at approximately 670 nm is typical for hypericins rich acetone extracts.

Determination of hypericins in the extract by UHPLC-MS/MS and UHPLC/PDA

Concentration of total hypericins in the methanol / acetone (2:1 w/w) extract were determined by both UHPLC-MS/MS and UHPLC/PDA methods independently. The analytical term “total hypericins” or “total naphthodianthrones” is often used in literature and it refers to the group of hypericin and its derivatives, which are the main constituents of dried plant material (Karioti and Bilia 2010; Williams et al. 2006). Hypericin derivatives include pseudohypericin, isohypericin and biosynthetic precursors protohypericin and protopseudohypericin. Concentration 182,5 ± 14,9 $mg \cdot g^{-1}$ of total hypericins in the dried *H. perforatum* extract was determined by the UHPLC-MS/MS method and 158,0 ± 38,2 $mg \cdot g^{-1}$ by the UHPLC/PDA method. The results correspond to 21,29, resp. 18,43 $mg \cdot g^{-1}$ of total hypericins in the herb dry matter. The results are in an acceptable correspondence. Chromatogram of UHPLC-MS/MS hypericin determination in the extract with quantification ion m/z 300 is shown in Fig. 6. The determined concentrations are relatively high, in comparison with results published by other authors. The range of total hypericins concentrations found by other authors in *H.*

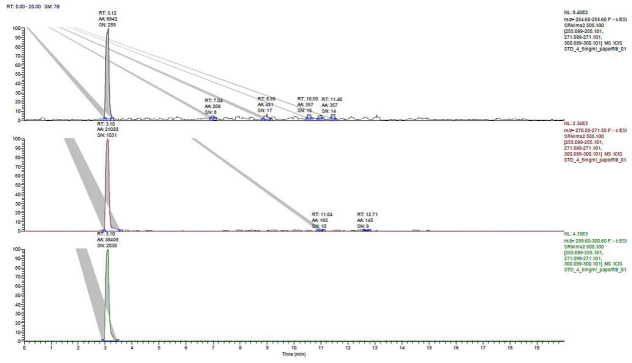

Fig. 6 UHPLC-MS/MS hypericin determination in the extract with quantification iont m/z 300

Fig. 7 PHB submicron fiber mat enriched by the *H. perforatum* extract prepared by the centrifugal spinning technology (left) and SEM image of microstucture of the fiber mat (right)

perforatum and other *Hypericum* species is very wide.

Southwell and Bourke (2001) found significant seasonal variation in hypericin content in a broad and narrow leaf biotypes of *H. perforatum* in New South Wales. Australia. In two consecutive seasons, the hypericin/pseudohypericin content in the broad leaf biotype varied from winter minimum of less than 100 ppm to a summer maximum approaching 3000 ppm. In contrast the narrow leaf biotype increased from similar winter values to summer maxima approaching 5000 ppm.

Çirak et al. (2008) found pseudohypericin concentrations ranged from traces to 2.94 mg·g^{-1} dry matter in *H. perforatum* from Northern Turkey. Hypericin and pseudohypericin concentrations in the range of 0.1 - 7 and 0.1 - 12 mg·g^{-1} were determined by other researchers (Bruni and Sacchetti 2009). These secondary metabolites were localised mainly in dark glands in leaf and petal margin. Generally, stems produced neither hypericin nor pseudohypericin (Ayan and Çirak 2008). Bagdonaitė E et al. 2010 summarised results of determination of hypericin and pseudohypericin in aerial parts at full flowering of *H. perforatum* of six different geographic origin. The results were in the range 0,1 - 6,6 mg·g^{-1} for hypericin and 0,1 - 16 mg·g^{-1} dry matter for pseudohypericin. Ramezani and Zamani (2017) extracted 5.105 mg of purified hypericins

Table 4 Singlet oxygen quantification by the DPIBF method in DMSO: corrected slopes k_{corr} and corresponding decomposition half-times $\tau_{1/2corr}$ (ar. average ± SD) of hypericin standard and *H. perforatum* extract against DPIBF control

Sample	k_{corr} (min^{-1})	$\tau_{1/2corr}$ (min)
Hypericin standard	0,148	5 ± 0,7
H. perforatum extract	0,0066	103 ± 11,3

per gram dried *H. perforatum* plant leaves. Optimization of hypericin extraction conditions from dried plant *H. perforatum* performed in ultrasonic bath and ethanol/methanol solvents mixture (1:1), was carried out by Tahmasebi-Boldaji et al. (2019). In the optimal conditions they found 0,112 mg·g^{-1} of hypericin in dry matter of the plants. Recently, content variability of bioactive secondary metabolites in *H. perforatum* in Italy was studied by Carrubba et al. (2021). Total naphtodianthrones content in 2016 was rather double than in 2015 (10,4 vs. 5,9 mg·g^{-1} d.m.), demonstrating the crucial influence of the higher temperatures experienced by plants in the blooming stage. However a strong effect of genotype was also fond, as many of the tested genotypes showed contrasting values in both years. Only the highest of the total contents of hypericins determined by different authors are in acceptable correspondence with our results. Except of the influence of genotype and local conditions discussed above, we have noticed a methodological malpractice in the analytical procedures, which can decrease the final results of the naphtodianthrones content determination. A lot of researchers use nylon filters to remove particular contamination form the extracts before HPLC analysis. However, we noticed strong red coloration of the nylon filter, used for the extract filtration, pointing to significant adsorption of naphtodianthrones on the nylon surface. That is why we used filtration paper instead the nylon filter.

Preparation of the PHB submicron fiber mat enriched by the extract and its characterization by SEM

Fig. 7 shows PHB submicron fiber mat enriched by the H. perforatum extract prepared by the centrifugal spinning technology and SEM image of microstructure of the fiber mat. Diameters of most of the fibers are in submicron area, but thicker fibers are present sporadically in the fiber mat, too.

Quantification of singlet oxygen production by the extract and the PHB submicron fiber mats enriched by the extract

Table 4 shows singlet oxygen quantification by the DPIBF

Table 5 Singlet oxygen quantification by the DPIBF method in hexan: corrected slope k_{corr} and corresponding decomposition half-times $\tau_{1/2corr}$ (ar. average ± SD) of PHB nanofiber membrane functionalized by *H. perforatum* extract against DPIBF control and pure PHB nanofiber membrane

k_{corr} (min^{-1})	$\tau_{1/2corr}$ (min)
0,0104	67 ± 2,4

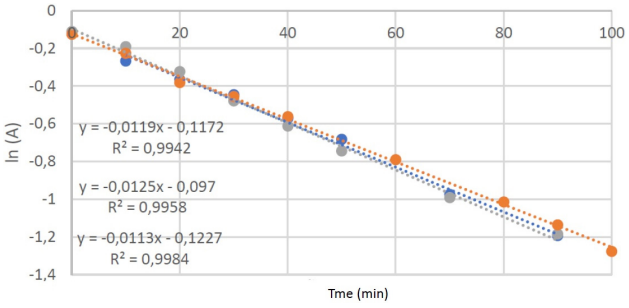

Fig. 8 DPIBF decline expressed as absororbance natural logarithm in time in the presence of the PHB fiber mat functionalized by *H. perforatum* extract

method in DMSO, expressed as corrected slopes k_{corr} and corresponding decomposition half-times $\tau_{1/2corr}$ of hypericin standard and *H. perforatum* extract against DPIBF control. The decomposition half-time $\tau_{1/2corr}$ of the *H. perforatum* extract is about twenty times lower than $\tau_{1/2corr}$ of the hypericin standard, because of lower hypericin concentration in the extract. Shielding effect of other components of the extract is also probable. However, singlet oxygen production by the raw *H. perforatum* extract is still very significant. Comparison of photocatalytic activities of hypericin with other compounds producing singlet oxygen in visible light, such as phtalocyanines, porphyrins, rose bengal, or bacteriochlorins, is difficult, because singlet oxygen quantum yields of photosensitizers differ when measured in different solvents. There is no single reference method to compare photocatalytic activities of the photocatalytic compounds. Values of corrected slope k_{corr} and corresponding decomposition half-times $\tau_{1/2corr}$ of PHB nanofiber membrane functionalized by *H. perforatum* extract against DPIBF control and pure PHB nanofiber membrane are shown in Table 5. DPIBF decline expressed as absorbance natural logarithm in time in the presence of the PHB fiber mat functionalized by *H. perforatum* extract in Fig. 8. We have found very significant production of singlet oxygen by the functionalized submicron fiber membrane.

Determination of the antibacterial activity of samples of the submicron fiber mat loaded with the extract

Results of determination of antibacterial activities of the control and *H. perforatum* extract loaded fiber mats against *Escherichia coli* are shown in Table 6. We have found a hundred percent sure antibacterial effect of the submicron fiber mat loaded with the hypericin-rich extract under visible light irradiation and even in the dark. *Esherichia coli* bacteria were selected for the experiment as a typical representative of gram-negative bacteria. Gram-negative bacteria are typically characterized by an impermeable outer cell membrane that contains endotoxins and blocks antibiotics, dyes, and detergents, protecting the sensitive inner membrane and cell wall. The outer membrane of gram-negative bacteria plays an important role that is related to resistance to many antibiotics that are highly effective against gram-positive bacteria. This explains the higher prevalence of gram-negative infections in the modern hospital environment (Sperandio et al. 2013). It was shown that cellular localization and cell death mechanisms (apoptosis and necrosis) are dependent on the cell type (de Andrade et al. 2021). (Nasim et al. (2013) found only negligible effect (< 0.2 log reduction) of photodynamic inactivation of *E. coli* bacteria. However, Zhang et al. (2018) evaluated the efficiency of hypericin based photodynamic therapy on *E. coli*, single factor experiments and

Table 6 Results of determination of antibacterial activities of the control and *H. perforatum* extract-loaded fiber mats against *Escherichia coli*

Sample	Time 0 h	Time 18 h	Antimicrobial activity R
Control fiber mat 0 lighted	U_0 = 3,9	U_t = 5,3	-
Control fiber mat - unlighted	U_0 = 3,9	U_t = 5,6	-
Functionalized fiber mat - lighted	-	A_t = 0	5,3
Functionalized fiber mat - unlighted	-	A_t = 0	5,6

U_0 is an arithmetic average of common logarithms of viable bacteria (CFU), determined with 3 control PHB samples immediately after inoculation. U_t is an arithmetic average of common logarithms of viable bacteria (CFU), determined with 3 control PHB membrane samples after 18 h of incubation. At is an arithmetic average of common logarithms of viable bacteria (CFU), determined with 3 experimental PHB - *H. perforatum* samples after 18 h of incubation. R is antibacterial activity calculated according to the formula: $R = (U_t - U_0) - (A_t - U_0) = U_t - A_t$

response surface optimization experiment were conducted to obtain the optimum parameter values. Data indicated that hypericin possessed a strong ability to bind with cells. In addition, a significant increase was observed in intracellular reactive oxygen species (ROS) level after hypericin-based photosensitization treatment. Therefore, hypericin-based photosensitization seems to be a promising method to efficiently inactivate *E. coli*. It is expected to be a safe, efficient, low cost and practical method which can be applied in the field of food safety.

According to the World Health Organization (WHO), one of the most significant challenges of the present century is bacterial resistance. Antimicrobial Photodynamic Therapy (aPDT) has been proposed as an alternative to avoid the use of drugs that lead to resistance. Strong potential of hypericin has been reported in aPDT to photoinactivate various species of microorganisms in planktonic form and biofilm. Our results contribute to such vision. Nanofiber membranes functionalized by hypericin rich extracts have a significant potential to be used for antimicrobial and antiviral air and water filters. Immobilized hypericins can be utilized for development of antimicrobial and antiviral surfaces, too.

Acknowledgement

This work was supported by the TACR project number TH03020466 and by the by METROFOOD-CZ project MEYS Grant No: LM2018100.

References

Abdelhamid S, Sharaf A, Youssef T, Kassab K, Salaheldin TA, Zedan AF (2020) Spectroscopic and photostability study of water-soluble hypericin encapsulated with polyvinyl-pyrrolidone. Biophys Chem 266:106454

Abdelsalam AM, Somaida A, Ambreen G, Ayoub AM, Tariq I, Engelhardt K, Garidel P, Fawaz I, Amin MU, Wojcik M, Bakowsky U (2021) Surface tailored zein as a novel delivery system for hypericin: Application in photodynamic therapy. Mater Sci Eng C 129:112420

Amjadi I, Mohajeri M, Borisov A, Hosseini MS (2019) Antiproliferative Effects of Free and Encapsulated Hypericum Perforatum L. Extract and Its Potential Interaction with Doxorubicin for Esophageal Squamous Cell Carcinoma. J Pharmacopuncture 22(2):102-108

Avato P, Guglielmi G (2008) Determination of Major Constituents in St. John's Wort Under Different Extraction Conditions. Pharm Biol 42(1):83-89

Avato P, Raffo F, Guglielmi G, Vitali C, Rosato A (2004) Extracts from St John's Wort and their antimicrobial activity. Phytother Res 18(3):230-232

Ayan AK, Çirak C (2008) Hypericin and Pseudohypericin Contents in Some Hypericum. Species Growing in Turkey, Pharm Biol 46(4):288-291

Ayane T, Peng S, Tsai H-C (2015) Drug Carrier for Photodynamic Cancer Therapy. Int J Mol Sci 16(9):22094-22136

Bagdonaitė E, Martonfi P, Repcak M, Labokas J (2010) Variation in the contents of pseudohypericin and hypericin in Hypericum perforatum from Lithuania. Biochem Syst Ecol 38(4):634-640

Balmeh N, Mahmoudi S, Mohammadi N, Karabedian A (2020) Predicted therapeutic targets for COVID-19 disease by inhibiting SARS-CoV-2 and its related receptors. Inform Med Unlocked 20:100407

Barras A, Boussekey L, Courtade E, Boukherroub R (2013) Hypericin-loaded lipid nanocapsules for photodynamic cancer therapy in vitro. Nanoscale 5: 10562-10572

Beran M, Drahorad J, Husek Z, Toman F (2017) A device for the production of nanofibres or microfibres from solutions, emulsions, liquid suspensions or melts containing a spinning substance. Czech Utility Model 30609

Birt D, Widrlechner M, Hammer K, Hillwig M, Wei J, Kraus G, Murphy P, Mccoy J-A, Wurtele E, Neighbors J, Wiemer D, Maury W, Price J (2009) Hypericum in infection: Identification of anti- viral and anti-inflammatory constituents. Pharm Biol 47:774-782

Bouron A, Lorrain E (2014) Cellular and molecular effects of the antidepressant hyperforin on brain cells: Review of the literature. Encephale 40(2):108-113

Bruni R, Sacchetti G (2009) Factors affecting polyphenol biosynthesis in wild and field grown St. John's Wort (Hypericum perforatum L. Hypericaceae/Guttiferae). Molecules 14(2):682-725

Carrubba A, Lazzara S, Giovino A, Ruberto G, Napoli E (2021) Content variability of bioactive secondary metabolites in Hypericum perforatum L. Phytochem Lett 46:71-78

Chen H, Ishfaq M, Zhang Y, Ren Y, Zhang R, Huang X, Diao L, Liu H, Li X, Sun X, Abbas G, Li G (2019) Antiviral Activity Against Infectious Bronchitis Virus and Bioactive Components of Hypericum perforatum L. Front Pharmacol 10:1272

Çirak C, Radusiene J, Janulis V, Ivanauskas L (2008) Pseudohypericin and Hyperforin in Hypericum perforatum from Northern Turkey: Variation among Populations, Plant Parts and Phenological Stages. J Integr Plant Biol 50(5):575-580

Conrado PCV, Sakita KM, Arita GS, Gonçalves RS, Cesar GB, Caetano W, Hioka N, Voidaleski MF, Vicente VA, Svidzinski TIE, Bonfim-Mendonça PS, Kioshima ES (2021) Hypericin-P123-photodynamic therapy in an ex vivo model as an alternative treatment approach for onychomycosis caused by Fusarium spp. Photodiagnosis Photodyn Ther 35:102414

Cossuta D, Vatai T, Báthori M, Hohmann J, Keve T, Simándi B (2012) Extraction of hyperforin and hypericin from St. John's wort (Hypericum perforatum L.) with different solvents. J

Food Process Eng 35(2):222-235
Cvetanovic Zobenica K, Lacnjevac U, Etinski M, Vasiljevic-Radovic D, Stanisavljev D (2019) Influence of the electron donor properties of hypericin on its sensitizing ability in DSSCs. Photochem Photobiol Sci 18:2023
Das S, Singha Roy A (2020) Naturally Occurring Anthraquinones as Potential Inhibitors of SARS- CoV-2 Main Protease: A Molecular Docking Study. ChemRxiv. Preprint 12245270
Datta S, Hovan A, Jutková A, Kruglik S, Jancura D, Miskovsky P, Bánó G (2018) Phosphorescence Kinetics of Singlet Oxygen Produced by Photosensitization in Spherical Nanoparticles. Part II. The Case of Hypericin-Loaded Low-Density Lipoprotein Particles. J Phys Chem B 122(20):5154-5160
Dayyih AA, Alawak M, Ayoub AM, Amin MU, Dayyih WA, Engelhardt K, Duse L, Preis E, Brüßler J, Bakowsky U (2021) Thermosensitive liposomes encapsulating hypericin: Characterization and photodynamic efficiency. Int J Pharm 609:121195
de Andrade GP, de Souza TFM, Cerchiaro G, Pinhal MADS, Ribeiro AO, Girão MJBC (2021) Hypericin in photobiological assays: An overview. Photodiagnosis Photodyn Ther 35:102343
Delcanale P, Hally C, Nonell S, Bonardi S, Viappiani C, Abbruzzetti S (2020) Photodynamic action of Hypericum perforatum hydrophilic extract against Staphylococcus aureus. Photochem Photobiol Sci 19:324-331
Draves A, Walker S (2003) Analysis of the hypericin and pseudohypericin content of commercially available St John's Wort preparations. Can J Clin Pharmacol 10(3):114-118
Eldeeb E, Belal A (2020) Two Promising Herbs that May Help in Delaying Corona Virus Progression. IJTSRD 4(4):2456-6470
Engelhardt V, Krammer B, Plaetzer, K (2010) Antibacterial photodynamic therapy using water- soluble formulations of hypericin or mTHPC is effective in inactivation of Staphylococcus aureus. Photochem Photobiol Sci 9:365-369
Galinari CB, Conrado PCV, Arita GS, Mosca VAB, Mělo RC, de Paula Bianchi T, Faria DR, Sakita KM, Malacarne LC, Gonçalves RS, de SouzaPereira PC, Cesar GB, Caetano W,Souza M, Palácios RS, Baesso ML, Svidzinski TIE, Cotica ÉSK, de Souza Bonfim-Mendonça P. (2021) Nano encapsulated hypericin in P-123 associated with photo dynamic therapy for the treatment of dermatophytosis. J Photochem Photobiol B 215:112103
Garcia I, Ballesta S, Gilaberte Y, Rezusta A, Pascual A (2015) Antimicrobial photodynamic activity of hypericin against methicillin-susceptible and resistant Staphylococcus aureus biofilms. Future Microbiol 10(3):347-356
Gharge D, Pavan T, Sunil B, Dhabale P (2009) Hyperforin as a natural antidepressant: an overview J Pharm Res 2(9): 1373-1375
Head C, Luu Q, Sercarz J, Saxton R (2006) Photodynamic therapy and tumor imaging of hypericin-treated squamous cell carcinoma. World J Surg Oncol 4:87
Hudson JB, Lopez-Bazzocchi I, Towers GH (1991) Antiviral activities of hypericin. Antiviral Res 15(2):101-12
Islam R, Parves MR, Paul AS, Uddin N, Rahman MS, Mamun AA, Hossain MN, Ali MA, Halim MA (2021) A molecular modeling approach to identify effective antiviral phytochemicals against the main protease of SARS-CoV-2. J Biomol Struct Dyn 39(9):3213-3224
Jacobson JM, Feinman L, Liebes L, Ostrow N, Koslowski W, Tobia A, Cabana BE, Lee D-H, Spritzler J, Prince AM (2001) Pharmacokinetics, safety, and antiviral effects of hypericin, a derivative of St. John's wort plant, in patients with chronic hepatitis C virus infection. Antimicrob Agents Ch 45:517-524
Jendzelovska Z, Jendzelovsky R, Kucharova B, Fedorocko P (2016) Hypericin in the Light and in the Dark: Two Sides of the Same Coin. Front Plant Sci 7:560
Johnston E, Trammell S, Goldston H, Conrad D (2001) Sensitization of nanoporous TiO2 electrodes using the naturally occurring chromophores: stentorin and hypericin. J Photochem Photobiol A 140:179-183
Kalogeropoulos N, Mourtzinos I, Yannakopoulou K, Gioxari A, Chiou A, Karathanos V (2008) Encapsulation of Hypericum perforatum (St John's wort) methanolic extract in β -cyclodextrin. Planta Med 74-PC37
Karioti A, Bilia AR (2010) Hypericins as potential leads for new therapeutics. Int J Mol Sci 11(2):562-594
Kim DE, Min JS, Jang MS, Lee JY, Shin YS, Park CM, Song JH, Kim HR, Kim S. Jin Y-H (2019) Natural Bis-Benzylisoquinoline Alkaloids-Tetrandrine, Fangchinoline, and Cepharanthine, Inhibit Human Coronavirus OC43 Infection of MRC-5 Human Lung Cells. Biomolecules 9(11):696
Kimmer D, Vincent I, Dudák J, Bergerova E, Petras D, Les J, Holba M, Kalhotka L, Mikulka P, Korinkova R, Kubac L (2012) Bacteria Deactivation and Removal from Wastewater and Polluted Air. Nanocon 2012 Conference proceedings, p. 402
Koturevic B, Adnadjevic B, Jovanovic J (2021) Comparative kinetic analysis of total hypericin extraction from Hypericum perforatum flowers carried out under simultaneous external field and cooling reaction system operational conditions. Chem Eng Res Des 165:106-117
Kubin A, Loew GH (2004) Novel preparation of hypericin bonded with poly-n-vinylamides. Patent EP1289562B1
Kubin A, Loew GH, Burner U, Jessner G, Kolbabek H, Wierrani F (2008) How to make hypericin water-soluble. Die Pharmazie 63:263-269
Lima A, Dal Pizzol C, Filippin Monteiro F, Creczynski-Pasa T, de Andrade G, Ribeiro A, Perussi JR (2013) Hypericin encapsulated in solid lipid nanoparticles: phototoxicity and photodynamic efficiency. J Photochem Photobiol B 125: 146-154
Liu C, Zhu X, Lu Y, Zhang X, Jia X, Yang T (2021) Potential treatment with Chinese and Western medicine targeting NSP14 of SARS-CoV-2. J Pharm Anal 11(3):272-277
Liu X, Feng Y, Jiang C, Lou B, Li Y, Liu W, Yao N, Gao M, Ji Y, Wang Q, Huang D, Yin Z, Sun Z, Ni Y, Zhang J (2015) Radiopharmaceutical evaluation of 131I-protohypericin as a necrosis avid compound. J Drug Target 23(5):417-426
Lopera A, Velásquez A, Patiño Linares I, de Almeida L, Fontana C, Garcia C, Graminha M (2020) Efficacy of photodynamic

therapy using TiO2 nanoparticles doped with Zn and hypericin in the treatment of cutaneous Leishmaniasis caused by Leishmania amazonensis. Photodiagnosis Photodyn Ther 30:101676

Lopez-Bazzocchi I, Hudson JB, Towers GH (1991) Antiviral activity of the photoactive plant pigment hypericin. Photochem Photobiol 54(1):95-98

Luksiene Z (2003) Photodynamic therapy: mechanism of action and ways to improve the efficiency of treatment. Medicina (Kaunas) 39(12):1137-1150

Malacrida AM, Cortez Dias VH, Silva AF, dos Santos AR, Cesar GB, Bona E, Zanetti Campanerut- Sá PA, Caetano W, Graton Mikcha JM (2020) Hypericin-mediated photoinactivation of polymeric nanoparticles against Staphylococcus aureus. Photodiagnosis Photodyn Ther 30:101737

Milosevic T, Solujic S, Sukdolak S (2007) In Vitro Study of Ethanolic Extract of Hypericum perforatum L. on Growth and Sporulation of Some Bacteria and Fungi. Turk J Biol 31(4):237-241

Miskovsky P (2002) Hypericin--a new antiviral and antitumor photosensitizer: mechanism of action and interaction with biological macromolecules. Curr Drug Targets 3(1):55-84

Morais Fl, Goncalves R, Braga G, Calori I, Pereira P, Batistela V, Caetano W, Hioka N (2020) Stable Dipalmitoylphosphatidylcholine (DPPC) Liposomes Coated with F127 Copolymer for Hypericin. Loading and Delivery. ACS Appl Nano Mater 3(5):4530-4541

Nasim K, Yasaman SB, Gholamreza ED (2013) Photodynamic effect of hypericin on the microorganisms and primary human fibroblasts, Photodiagnosis Photodyn Ther 10(2):150-155

O'Neill JF, Wilson M, Wainwright M (2003) Comparative antistreptococcal activity of photobactericidal agents. J. Chemother 15(4):329-334

Onoue S, Seto Y, Ochi M, Inoue R, Ito H, Hatano T, Yamada S (2011) In vitro photochemical and phototoxicological characterization of major constituents in St. John's Wort (Hypericum perforatum) extracts. Phytochemistry 72(14-15): 1814-1820

Pitsillou E, Liang J, Karagiannis C, Ververis K, Darmawan KK, Ng, K, Hung A, Karagiannis TC (2020a) Interaction of small molecules with the SARS-CoV-2 main protease in silico and in vitro validation of potential lead compounds using an enzyme-linked immunosorbent assay. Comput Biol Chem 89:107408

Pitsillou E, Liang J, Ververis K, Lim KW, Hung A, Karagiannis TC (2020b) Identification of Small Molecule Inhibitors of the Deubiquitinating Activity of the SARS-CoV-2 Papain-Like Protease: in silico Molecular Docking Studies and in vitro Enzymatic Activity Assay. Front Chem 8:1171

Pourhojat F, Shariati S, Sohrabi M, Mahdavi H, Asadpour L (2018) Preparation of antibacterial electrospun Polylactic-co-glycolic acid nanofibers containing Hypericum Perforatum with bedsore healing property and evaluation of its drug release performance. Int J Nano Dimens 9(3):286-297

Pourhojat F, Sohrabi M, Shariati S, Mahdavi H, Asadpour L (2017) Evaluation of poly ε-caprolactone electrospun nanofibers loaded with Hypericum perforatum extract as a wound dressing. Res Chem Intermed 43:297

Pu X-Y, Liang J-P, Wang X-H, Xu T, Hua L.-Y, Shang R, Liu Y, Xing Y-M (2009) Anti-influenza A virus effect of Hypericum perforatum L. extract. Virol Sin 24:19

Punegov VV, Kostromin VI, Fomina MG, Zaynullin VG, Yushkova EA, Belyh DV, Chukicheva IU, Zaynullin GG (2015) Microwave-assisted extraction of hypericin and pseudohypericin from Hypericum perforatum. Russ J Bioorg Chem 41:757-761

Ramezani Z, Zamani M (2017) A Simple Method for Extraction and Purification of Hypericins from St John's Wort. Jundishapur J Nat Pharm Prod 12(1):e13864

Rezusta A, López-Chicón P, Paz-Cristobal MP, Alemany-Ribes M, Royo-Díez D, Agut M, Semino C, Nonell S, Revillo MJ, Aspiroz C, Gilaberte Y (2012) In vitro fungicidal photodynamic effect of hypericin on Candida species. Photochem Photobiol 88(3):613-619

Roslaniec M, Weitman H, Freeman D, Mazur Y, Ehrenberg B (2000) Liposome binding constants and singlet oxygen quantum yields of hypericin, tetrahydroxy helianthrone and their derivatives: studies in organic solutions and in liposomes. J Photochem Photobiol B, 57(2-3):149-158

Saddiqe Z, Naeem I, Maimoona A (2010) A review of the antibacterial activity of Hypericum perforatum L. J Ethnopharmacol 131(3):511-521

Schempp CM, Pelz K, Wittmer A, Schöpf E, Simon JC (1999) Antibacterial activity of hyperforin from St John's wort, against multiresistant Staphylococcus aureus and gram-positive bacteria. The Lancet 353(9170):2129

Schmitt AC, Ravazzolo A, Poser G (2001) Investigation of some Hypericum species native to Southern Brasil for aniviral aktivity. J Ethnopharmacol 77:239-245

Schwob I, Bessière JM, Viano J (2002) Composition of the essential oils of Hypericum perforatum L. from southeastern France. C R Biol 325:781-785

Sepúlveda AAL, Arenas Velásquez AM, Patiño Linares IA, de Almeida L, Fontana CR, Garcia C, Graminha MAS (2020) Efficacy of photodynamic therapy using TiO2 nanoparticles doped with Zn and hypericin in the treatment of cutaneous Leishmaniasis caused by Leishmania amazonensis. Photodiagnosis Photodyn Ther 30:101676

Severyukhina AN, Petrova NV, Yashchenok AM, Bratashov DN, Smuda K, Mamonova IA, Yurasov NA, Puchinyan DM, Georgieva R, Bäumler H, Lapanje A, Gorin DA (2017) Light-induced antibacterial activity of electrospun chitosan-based material containing photosensitizer. Mat Sci Eng: C 70:311

Smith M, Smith JC (2020) Repurposing Therapeutics for COVID-19: Supercomputer-Based Docking to the SARS-CoV-2 Viral Spike Protein and Viral Spike Protein-Human ACE2 Interface. ChemRxiv. Preprint 11871402

Southwell IA, Bourke CA (2001) Seasonal variation in hypericin content of Hypericum perforatum L. (St. John's Wort). Phytochemistry 56(5):437-441

Sperandio FF, Huang YY, Hamblin MR (2013). Antimicrobial photodynamic Therapy to kill Gram-negative bacteria. Recent Pat Antiinfect Drug Discov 8(2):108-120

Srikanth B, Goutham R, Badri Narayan R, Ramprasath A, Gopinath KP, Sankaranarayanan AR (2017) Recent advancements in supporting materials for immobilised photocatalytic applications in waste water treatment J Environ Manage 200:60-78

Sytar O, Svediene J, Loziene K, Paskevicius A, Kosyan A, Taran N (2016) Antifungal properties of hypericin, hypericin tetrasulphonic acid and fagopyrin on pathogenic fungi and spoilage yeasts. Pharm Biol 54(2):3121-3125

Tahmasebi-Boldaji R, Hatamipour M, Khanahmadi M, Sadeh P, Najafipour I (2019) Ultrasound- assisted packed-bed extraction of hypericin from Hypericum perforatum L. and optimization by response surface methodology. Ultrason Sonochem 57:89-97

Tatsis EC, Boeren S, Exarchou V, Troganis AN. Vervoort J, Gerothanassis IP (2007) Identification of the major constituents of Hypericum perforatum by LC/SPE/NMR and/or LC/MS. Phytochemistry 68(3):383-393

Umek A, Kreft S, Kartnig T, Heydel B (1999) Quantitative phytochemical analyses of six hypericum species growing in Slovenia. Planta Med 65:388-390

Varchola J, Želonková K, Chorvat D, Jancura D, Miškovský P, Bánó G (2016) Singlet oxygen produced by quasi-continuous photo-excitation of hypericin in dimethyl-sulfoxide. J Lumin 177:17-21

Williams FB, Sander LC, Wise SA, Girard J (2006) Development and evaluation of methods for determination of naphthodianthrones and flavonoids in St. John's Wort. J Chromatogr A 1115(1):93-102

Wirz A, Meier B, Sticher O (2001) Stability of hypericin and pseudohypericin in extract solutions of Hypericum perforatum and in standard solutions. Pharm Ind 63(4):410-415

Yow CM, Tang HM, Chu ES, Huang Z (2012) Hypericin-mediated photodynamic antimicrobial effect on clinically isolated pathogens. Photochem Photobiol 88(3):626-632

Zanoli P (2004) Role of hyperforin in the pharmacological activities of St. John's Wort. CNS Drug Rev 10(3):203-218

Zhang J, Zhang F, Tang Q-J, Xu C, Meng X (2018) Effect of photodynamic inactivation of Escherichia coli by hypericin. World J. Microbiol. Biotechnol. 34, article number 100

Zugle R, Antunes E, Khene S, Nyokong T (2012) Photooxidation of 4-chlorophenol sensitized by lutetium tetraphenoxy phthalocyanine anchored on electrospun polystyrene polymer fiber. Polyhedron 33(4):74-81